Nuclear Instruments and Methods in Physics Research B xxx (2007) xxx–xxx

NIM B Beam Interactions with Materials & Atoms

www.elsevier.com/locate/nimb

# Installation of ion implantation beam line for 3 MV Tandem Pelletron

P.R. Poudel *, L.J. Mitchell, E.B. Smith, L.C. Phinney, K. Hossain, L.R. Burns, D.L. Weathers, J.L. Duggan, F.D. McDaniel

*Ion Beam Modification and Analysis Laboratory, Department of Physics, University of North Texas, 211 Avenue A, Denton, TX 76203, United States*

Available online

**Abstract**

An MeV energy beam line for ion implantation of carbon and silicon to fashion optically-active nanocrystals has been constructed at the Ion Beam Modification and Analysis Laboratory at the University of North Texas (UNT). The implantation line is at 15° and consists of a set of slits to define the beam, a doublet quadrupole focusing lens, a 40 kV electrostatic ion beam raster scanner and target chamber for 2 cm diameter circular implants. A 1.95 m drift section between the scanner and target is sufficient to accommodate 10 MeV carbon and silicon ions. It was determined that the separation between the slits and quadrupole should be at least 10 cm to achieve point-to-parallel focusing in the beam line. It was also determined that, for a slit opening of 2 mm, the distance between the upstream bending magnet and the analyzing slit should be at least 20 cm to allow only single isotopes of carbon to pass into the beam line.

© 2007 Elsevier B.V. All rights reserved.

*PACS:* 81.o5.UW; 61.72.Tt; 29.27.Bd; 27.27.−a

*Keywords:* Implantation; Carbon; Silicon; Raster scanner; Quadrupole; Charge state

## 1. Introduction

High energy ion implantation/irradiation has found some interesting uses in the semiconductor industry, predominantly as a research tool, and in the radiation therapy industry for treating certain type of cancers. For research and the limited applications where cost is not the driving issue, high energy ion implantation/irradiation has had some success. For example, since the dose can be tightly controlled, high energy irradiation has been successful in simulating the effects of radiation [1] on microelectronic devices [2,3] and biological materials, with both terrestrial and space applications.

More recently researchers have been exploring the possibility of using high energy ion implantation/irradiation for use in nanofabrication. Some researchers are taking a focused beam approach [4], while others are using a more standard rastered beam technique that utilizes the damaging effects and annealing power of energetic ions to precipitate nanoclusters [5]. The installation of a low-MeV implant line at the University of North Texas's, Ion Beam Modification and Analysis Laboratory follows the traditional raster beam approach. This facility will primarily be used to fabricate nanocrystals under the bombardment of energetic ions, but will also be instrumental in ion irradiation research and deep impurity implantations. In what follows, we discuss the design and installation of this beam line, with particular emphasis on the consideration given to determine the optimal placement of the various ion optical elements in the beam line given the constraints of our system.

## 2. Experimental set up

The line has been designed principally for implantation of carbon and silicon ions of up to 10 MeV. The implantation line shown schematically in Fig. 3, is 15° off the unde-

* Corresponding author. Tel.: +1 940 565 2223; fax: +1 940 565 2227.
*E-mail address:* prp0020@unt.edu (P.R. Poudel).

0168-583X/$ - see front matter © 2007 Elsevier B.V. All rights reserved.
doi:10.1016/j.nimb.2007.04.241



UNCORRECTED PROOF

flected beam line from the tandem accelerator. Ions from the accelerator are directed into the line by a High Voltage Engineering Corporation (HVEC) magnet that doubles as both a switching and an analyzing magnet. The implantation line is equipped with horizontal and vertical slits located immediately after the magnet, followed by a quadrupole doublet lens for focusing, a faraday cup for current measurement, a 40 kV National Electrostatic Corporation electrostatic ion beam raster scanner, and a target chamber for 2 cm diameter circular implants.

The beam line slits define the size of the beam, and the vertical slit also serves as the analyzing slit for the bending magnet. The position of slit has to be such that only one isotope can pass through at a time, while also allowing sufficiently high beam transmission. The distance of the slits from the bending magnet was determined from the angles of deflection of the two most abundant isotopes of carbon and silicon. These angles were determined by using the condition that different isotopes travel approximately equal distance through the magnet, or $R^{\mathrm{I}}\theta^{\mathrm{I}} = R\theta$, where $R^{\mathrm{I}}$ and $R$ are the radii of curvature and, $\theta^{\mathrm{I}}$ and $\theta$ are the angles of deflection for two different isotopes. The ratio of the radii of curvature in the worst case, which was for $\mathrm{C}^+$, was found from $\frac{R^{\mathrm{I}}}{R} = \sqrt{\frac{m+\Delta m}{m}} = 1.040$, where $\Delta m$ is the mass difference, $m$ is the mass of $^{12}\mathrm{C}$, or 12u and $m^{\mathrm{I}} = m + \Delta m = 13.003\mathrm{u}$. For an angle of deflection of $\theta = 15$ for $^{12}\mathrm{C}$, the difference between the deflection angles for the two isotopes was found to be 0.55°. The minimum distance of slit from the magnet that cuts off one isotope and allows the other isotope to pass through was thus determined to be 25 cm for a slit width of 2 mm. The geometry to fix the separation between the bending magnet and the slit is shown schematically in Fig. 1. The placement location of the downstream quadrupole doublet lens to focus the beam coming from the slits was determined by applying the conditions for point-to-parallel focusing. This involved using standard transfer matrix techniques for paraxial beams [6]. Specifically, the generic transport matrices used to solve for the point-to-parallel focusing are the drift transform matrix $D_r[z] = \begin{pmatrix} 1 & z \\ 0 & 1 \end{pmatrix}$, and the focus transform matrix $F[k,z] = \begin{pmatrix} \cos[kz] & k^{-1}\sin[kz] \\ -k\sin[kz] & \cos[kz] \end{pmatrix}$ and defocus transform matrix $D[k,z] = \begin{pmatrix} \cosh[kz] & k^{-1}\sinh[kz] \\ k\sinh[kz] & \cosh[kz] \end{pmatrix}$ for a quadrupole lens [6]. Here, $k = \sqrt{\frac{V_{\mathrm{qdr}}}{G_0^2 E_{\mathrm{beam}}/q}}$, where $V_{\mathrm{qdr}}$ is the quadrupole potential, $G_0$ is the lens gap radius, $E_{\mathrm{beam}}$ is the ion energy, $q$ is the ion charge; $z$ is the distance along the beam axis from the beginning of the region described by a particular matrix. The overall horizontal ($X$) and vertical ($Y$) transport matrices from the slits to the end of the quadrupole doublet are given by $X_{\mathrm{tot}} = D[k_2,w] \cdot D_r[-D_1] \cdot F[k_1,w] \cdot D_r[L_1]$, respectively, where $L_1$ is the distance from the slits to the entrance of the quadrupole, $w$ is the length of each quadrupole singlet, $D_1$ is the distance between the singlets, and $k_1$ and $k_2$ are the $k$ values for the first and second singlets, respectively. The condition for point-to-parallel focusing is that the second row, second column elements of both $X_{\mathrm{tot}}$ and $Y_{\mathrm{tot}}$ vanish. Mathematica was used to solve these two equations simultaneously for $k_1$ and $k_2$ for different values of $L_1$ to accommodate our maximum quadrupole potential of $V_{\mathrm{qdr}} = 40$ kV, using $G_0 = 1.6$ cm and $w = 26.0$ cm. When $L_1$ was set to 10.0 cm for 6 MeV $^{12}\mathrm{C}^+$, the larger of the two $k's$ was found to be 4.8 corresponding to $V_{\mathrm{qdr}}$ close to 40 kV. Thus, any spacing between slits and quadrupole greater than 10 cm would have been satisfactory for achieving the point-to-parallel focusing. Because of other physical constraints, we chose 35.0 cm as the distance between the slits and quadrupole lens.

The raster scanner was installed immediately behind the quadrupole doublet. Electrostatic kinematic equations allowed us to determine the distance between the high vacuum target chamber and raster deflector, shown schematically in Fig. 2. Here, $d_1$ is the length of the scanner deflecting plate, $d_2$ is the distance from the scanner to the target, $h$ is the separation between the two deflecting plates, $h_1$ is the vertical beam deflection just after the beam leaves the deflector, and $h_2$ is the radius of the circular implant region. In between the electrodes (deflecting plates), the acceleration of the ion transverse to the beam axis is $a = \frac{qE}{m}$, where $q$ is the ion charge, $E$ is electric field between the plates and $m$ is the mass of the ion. Assuming zero initial transverse velocity, the time that the beam takes to deflect a vertical distance $h_1$ is $t = \sqrt{2h_1/a}$. The time to travel the length of deflecting plates is $d_1\sqrt{\frac{m}{2K}}$, where $K$ is the ion beam energy for the specified charge state. The time that the beam takes to travel $d_1$ (the horizontal distance) and the time it takes to travel $h_1$ (the vertical distance) are set to be equal in order to sweep the ion completely off the implanted region at minimum potential. This condition yields $h_1 = \frac{d_1^2}{2}\left(\frac{qE}{2K}\right)$, which leads to the result $d_2 = \frac{4h_2K}{qEd_1}$

UNCORRECTED PROOF

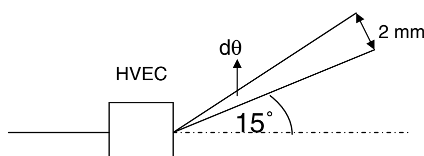


Fig. 1. Schematic illustration of the geometry to fix the slit distance from HVEC magnet.

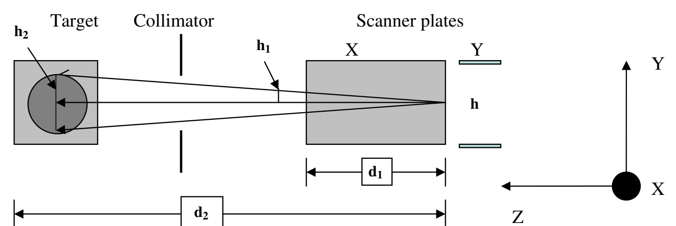


Fig. 2. Schematic illustration of the geometry to fix the drift length $d_2$.

Please cite this article in press as: P.R. Poudel et al., Installation of ion implantation beam line for 3 MV Tandem Pelletron, Nucl. Instr. and Meth. B (2007), doi:10.1016/j.nimb.2007.04.241

Table 1
Table showing the raster voltage for different carbon beam energy

| Rasterer voltage (kV) | Energy (MeV) | Ion charge (most probable charge) probability 62–89% |
|---|---|---|
| 4 | 1 | 2e |
| 5 | 2 | 3e |
| 7 | 3 | 3e |
| 9 | 4 | 3e |
| 8 | 5 | 4e |
| 15 | 10 | 5e |

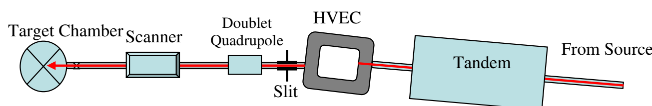


Fig. 3. Schematic diagram for ion implantation beam line for 3 MV Tandem Pelletron at UNT.

using the geometrical condition $\frac{d_2}{h_2} = \frac{d_1}{h_1}$. In terms of the plate separation and the applied voltage between the plates, the above expression becomes $d_2 = \frac{4h_2hK}{qVd_1}$. This calculation was made to figure out the value of $d_2$ for different beam energies and charge states, using a deflection plate length $d_1$ of 13.0 cm, plate separation $h$ of 4.0 cm and circular implant radius $h_2$ of 1.0 cm. Because of limitations imposed by the availability of lab space and size of equipment used. We fixed the drift distance between scanner and target at 1.95 m which easily accommodates a 10 MeV $^{12}C^{4+}$carbon beam (4+ being the most probable charge state emerging from the accelerator at terminal potential of 2 MV [7,8]) using a scanner electrode voltage of 15 kV. For 1.0 cm radius circular implants, Table 1 shows the required voltages across the rasterer for different carbon beam energies to accommodate the 1.95 m drift distance to the target. During assembly of the beam line, a laser and transit were used to align the various elements. Because the beam line is very long, the alignment was done in steps, each covering a small portion of the overall length (see Fig. 3).

To test the beamline's performance, the laboratory's Source of Negative Ions by Cesium Sputtering (SNICS) was used to produce a carbon beam to inject into a 3 MV 9SDH-2 Tandem Pelletron accelerator which has stable high energy for heavy ions ($\Delta E/E \sim 10^{-4}$) [9]. A cryopump and a turbo pump backed by a mechanical pump were used to pump down the beam line to a pressure of about $1 \times 10^{-7}$ torr. Convectron and ion gauges were used to monitor the pressure at the middle of beam line and at the target chamber. Faraday cups right after the quadrupole doublet and at the target chamber were used to monitor the beam current.

## 3. Result and discussion

The focused carbon beam of size $4 \times 4$ mm was achieved. The current of about 20 μA was obtained for the carbon beam of energy 1 MeV for double charge state under the vacuum pressure of $1.8 \times 10^{-7}$ torr. The ability to produce a negative ion, which is dependent on the electron affinity, will surely limit the materials that can be implanted. For those that do not have a substantial electron affinity such as nitrogen, a molecular ion may be chosen. For high fluence implants (>$10^{17}$ atoms/cm$^2$), only the strongest current producing materials may be used, if the implant time is to be reasonable. Information on cathode materials and achievable currents may be found in the following Refs. [10,11]. Initial tests indicate it is relatively simple to achieve 1–2 μA of carbon or silicon, depending on the desired charge state and energy. To anneal nanoclusters using an ion irradiation technique, fluences on the order of $10^{15}$ atoms/cm$^2$ are required [5]. For example, a 1 μA beam would correspond to an implant time of about 8 min for a fluence of $10^{15}$ atoms/cm$^2$. This current is more than sufficient to anneal nanocrystals and simulate most radiation dose scenarios. While small, the circular implant area (3.24 cm$^2$) is sufficient to produce research samples that can be analyzed or further processed. Currently, a target holder utilizing a rubber *o*-ring is used for easy removal of the implant samples. Typical target chamber pressures are on the order of $10^{-7}$ torr, but can be lower if a conflat setup is used.

## Acknowledgement

This work done at UNT was partially supported by Robert A. Welch foundation.

## References

[1] K. Yasuda, R. Ishigami, M. Sasase, S. Hatori, K. Ohashi, S. Tanaka, A. Yamamoto, Nucl. Instr. and Meth. B 191 (2002) 530.
[2] B.N. Guo, M. El Bouanani, S.N. Renfrow, D.S. Walsh, B.L. Doyle, J.L. Duggan, F.D. McDaniel, AIP Conf. Proc. 576 (2001) 531.
[3] J.R. Schwank, P.E. Dodd, M.R. Shaneyfelt, G. Vizkelethy, B.L. Draper, T.A. Hill, D.S. Walsh, G.L. Hash, B.L. Doyle, F.D. McDaniel, IEEE Trans. Nucl. Sci. 49 (2002) 2937.
[4] F. Watt, Nucl. Instr. and Meth. B 158 (1999) 165.
[5] D. Ila, R.L. Zimmerman, C.I. Muntele, P. Thevenard, F. Orucevic, C.L. Santamaria, P.S. Guichard, S. Schiestel, C.A. Carosella, G.K. Hubler, D.B. Poker, D.K. Hensley, Nucl. Instr. and Meth. B 191 (2002) 416.
[6] Hermann Wollnik, Optics of Charged Particles, Academic Press, Inc., Orlando, Florida, 1987.
[7] R.O. Sayer, L.B. Maddox, Compilation of Equilibrium Charge State Distribution Data, unpublished technical note, January 19, 1977.
[8] R.O. Sayer, Revue de Physique Appliquee 12 (1977) 1543, in: Proc. 2nd Int. Conf. on Electrostatic Accel. Technology, Strasbourg, France, May 24–27, 1977.
[9] F.D. McDaniel, J.L. Duggan, C. Yang, B.N. Guo, M. El Bouanani, M. Nigam, Nucl. Instr. and Meth. B 181 (2001) 99.
[10] National Electrostatics Corporation (NEC), Instruction Manual SNICS II Ion Source, Middleton Wisconsin, 1985.
[11] R. Middleton, A Negative Ion Cookbook, HTML version: M. Wiplich, <http://tvdg10.phy.bnl.gov/COOKBOOK>, October 1989.

UNCORRECTED PROOF

Please cite this article in press as: P.R. Poudel et al., Installation of ion implantation beam line for 3 MV Tandem Pelletron, Nucl. Instr. and Meth. B (2007), doi:10.1016/j.nimb.2007.04.241